

Solid-state Fluorescence Emission and Second-Order Nonlinear Optical Properties of Coumarin-based Fluorophores

Yi-Feng Sun · He-Ping Wang · Zhi-Yong Chen ·
Wen-Zeng Duan

Received: 11 July 2012 / Accepted: 24 August 2012 / Published online: 2 September 2012
© Springer Science+Business Media, LLC 2012

Abstract Some coumarin-based fluorophores were synthesized and characterized by elemental analysis, ^1H NMR, ^{13}C NMR and MS. The solid-state photoluminescence properties were studied. The benzocoumarins display interesting solid-state emission properties with an emission at wavelengths ranging from 532 to 645 nm, when excited by a 325 nm helium–cadmium laser at room temperature. The results demonstrated that the luminescent colors can be tuned from green to red by simply varying molecular structure. The benzocoumarin-phenyl boronic acid hybrid, 4-(3-oxo-3-(2-oxo-2*H*-1-naphtho[2,1-*b*]pyran-3-yl)-prop-1-enyl)phenyl boronic acid, showed obvious fluorescence response to water. Whereas the free compound was very weakly fluorescent in tetrahydrofuran (THF), the addition of water leads to an appearance of strong blue-green fluorescence and a dramatic increase of emission intensity. Besides, 3-(3-(3,4,5-trimethoxyphenyl)-prop-2-enyl)-2*H*-1-benzopyran-2-one exhibited second order nonlinear optical response to laser pulses. A noticeable second harmonic generation (SHG) under pulsed excitation at 1064 nm was observed. Preliminary nonlinear measurements on powder samples showed that the second harmonic generation efficiency is roughly 5.8 times that of potassium dihydrogen phosphate (KDP).

Keywords Coumarin · Chalcones · Phenylboronic acid · Aggregation-induced emission enhancement · Synthesis · Nonlinear optical property

Introduction

As an important class of organic heterocycles, coumarin derivatives have been widely reported to exhibit various biological activities [1–3], especially with regard to antioxidant and anti-inflammatory activities. Further, coumarin derivatives also show outstanding optical properties, which render them useful across a wide variety of applications such as optical brighteners, laser dyes, nonlinear optical chromophores, electroluminescent materials, solar energy collectors, two-photon absorption (TPA) materials, as well as fluorescent labels and probes in biology and medicine [4–9]. Additionally, certain coumarin dyes have been used as blue, green and red dopants in organic light-emitting diodes (OLED).

Chalcones, characterized by a three-carbon α,β -unsaturated carbonyl system, are found to be effective photosensitive materials, and exhibit promising nonlinear optical (NLO) properties [10]. Of particular interest, chalcones have also shown an impressive array of pharmacological activities [11].

Recently, we have reported the synthesis, crystal structures and optical properties of some coumarin derivatives [12–14]. As a part of our ongoing search project directed toward the synthesis and optical evaluation of novel coumarin derivatives, the present study concerns the synthesis and the solid state photoluminescence properties of eight coumarin-chalcone chromophores. Specially, two coumarin-chalcone boronic acid compounds are prepared in view of the fact that some boronic chalcone analogues have been

Y.-F. Sun · H.-P. Wang · Z.-Y. Chen
Guangdong Provincial Public Laboratory of Analysis and
Testing Technology, China National Analytical Center,
Guangzhou 510070, People's Republic of China

Y.-F. Sun (✉) · W.-Z. Duan
School of Chemistry and Chemical Engineering,
Taishan University,
Taian 271021, People's Republic of China
e-mail: sunyf50@yahoo.com.cn

used as fluorescent probes [15]. It was envisaged that these two multifunctional molecules consisting of coumarin, chalcone and boronic acid moieties in a single molecule may show unique optical properties. The structures of target molecules are shown in Fig. 1.

Experimental

General

All reagents and chemicals are commercially available and used without further purification. The melting points were determined with a WRS-1A melting point apparatus and are uncorrected. ^1H NMR and ^{13}C NMR spectra were taken on a Bruker AVANCE-300 NMR spectrometer and chemical shifts expressed as δ (ppm) values with TMS as internal standard. Element analysis was taken with a Perkin-Elmer 240 analyzer. Mass spectra (MS) were measured on a VG ZAB-HS or Agilent LC/MSD Trap XCT mass spectrometer. Absorption spectra were determined on a Hitachi U-3900 UV-Vis scanning spectrophotometer. The solution phase photoluminescence spectra were determined with a Hitachi F-2500 spectrometer and the slit widths were 5 nm for both excitation and emission. The solid-state photoluminescence spectra were measured using a Horiba Jobin-Yvon LabRam HR UV-NIR Confocal Laser MicroRaman spectrometer under a 325 nm helium-cadmium laser excitation. The second order nonlinear optical properties of **1d** was studied by the Kurtz powder method using a Q-switched Nd: YAG laser (Continuum Inc., USA) of 1064 nm wavelength, repetition rate of 10 Hz, 8 ns pulse width.

Synthesis of the Coumarin-Chalcone Derivatives (**1**)

The coumarin-based fluorophores were readily synthesized according to the method reported by us previously [12].

5-(3-oxo-3-(2-oxo-2H-1-naphtho[2,1-b]pyran-3-yl)-prop-1-enyl)-2-thiophene boronic acid (**1a**)

A mixture of 3-acetyl-2H-1-naphtho[2,1-b]pyran-2-one (**ANPO**) (476 mg, 2 mmol), 5-formyl-2-thiopheneboronic acid (310 mg, 2 mmol) and piperidine (0.5 mL) in anhydrous ethanol (30 mL) was heated under reflux for 5 h. After cooling, the solvent was removed under reduced pressure and the solid residues were recrystallized from ethanol to give brown solid, yield 65 %; mp 167–169 °C; ^1H NMR (300 MHz, $\text{DMSO-}d_6/\text{TMS}$) δ : 7.21 (dd, $J=5.1, 3.6$ Hz, 1H), 7.53 (d, $J=15.6$ Hz, 1H), 7.62–7.68 (m, 3H), 7.75–7.83 (m, 2H), 8.01 (d, $J=15.6$ Hz, 1H), 8.08 (d, $J=7.8$ Hz, 1H), 8.32 (d, $J=9.0$ Hz, 1H), 8.63 (d, $J=8.4$ Hz, 1H), 9.30 (s, 1H). ^{13}C NMR (75 MHz, $\text{DMSO-}d_6/\text{TMS}$) δ : 112.64, 116.46, 122.41, 123.14, 123.84, 126.45, 128.87, 129.01, 129.24, 129.84, 130.74, 133.65, 135.88, 136.89, 139.74, 142.57, 155.06, 158.58, 186.28. FAB-MS m/z : 377 ($\text{M} + \text{H}$)⁺. Anal. calcd for $\text{C}_{20}\text{H}_{13}\text{BO}_5\text{S}$: C 63.86, H 3.48; found: C 63.93, H 3.59.

4-(3-oxo-3-(2-oxo-2H-1-naphtho[2,1-b]pyran-3-yl)-prop-1-enyl) phenyl boronic acid (**1b**)

A mixture of **ANPO** (476 mg, 2 mmol), 4-formylphenylboronic acid (300 mg, 2 mmol) and piperidine

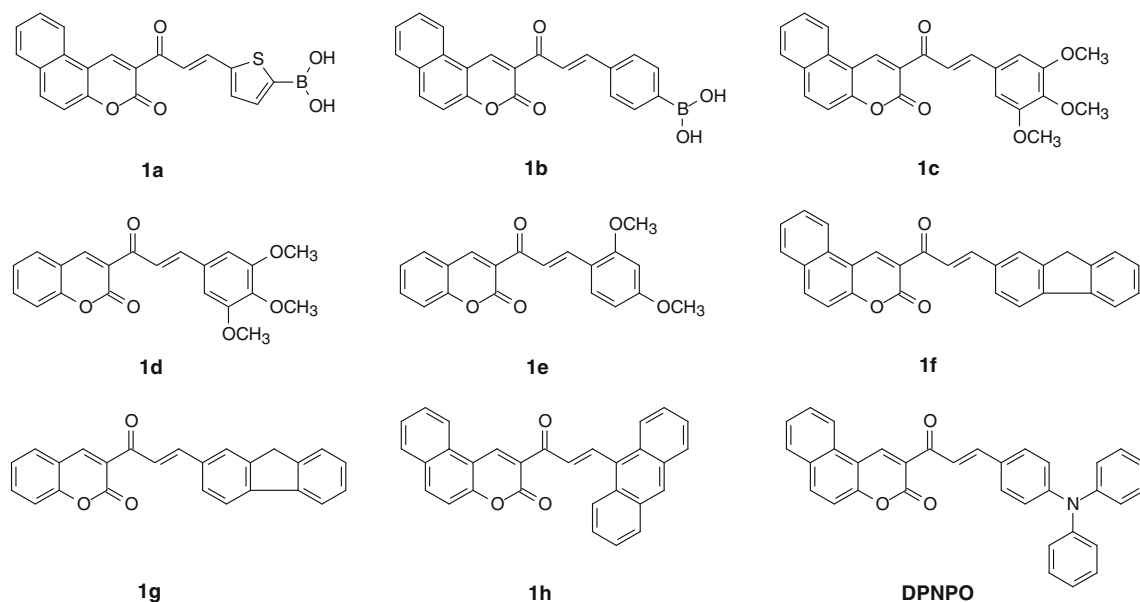


Fig. 1 The molecular structures of the coumarin-based fluorophores

(0.5 mL) in anhydrous ethanol (30 mL) was heated under reflux for 5 h. After cooling, the solvent was removed under reduced pressure and the solid residues were recrystallized from ethanol to give yellow solid, yield 61 %; mp >250 °C; ^1H NMR (300 MHz, DMSO- d_6 /TMS) δ : 7.54–7.69 (m, 2 H), 7.71–7.83 (m, 5 H), 7.88 (d, J =8.1 Hz, 2 H), 8.12 (d, J =8.4 Hz, 1 H), 8.23 (s, 2 H), 8.36 (d, J =9.0 Hz, 1 H), 8.70 (d, J =8.4 Hz, 1 H), 9.37 (s, 1 H). ^{13}C NMR (75 MHz, DMSO- d_6 /TMS) δ : 113.18, 117.05, 123.06, 124.85, 125.66, 127.00, 128.15, 129.50, 129.55, 129.81, 130.42, 135.15, 136.32, 136.37, 142.98, 144.56, 155.56, 158.92, 187.88. ESI-MS m/z : 371.0 (M + H) $^+$. Anal. calcd for C₂₂H₁₅BO₅: C 71.38, H 4.08; found: C 71.32, H 4.15.

3-(3-(3,4,5-trimethoxyphenyl)-prop-2-enoyl)-2H-1-naphtho[2,1-b]pyran-2-one (1c)

A mixture of ANPO (476 mg, 2 mmol), 3,4,5-trimethoxybenzaldehyde (392 mg, 2 mmol) and piperidine (0.5 mL) in anhydrous ethanol (30 mL) was heated under reflux for 5 h. After cooling, the solvent was removed under reduced pressure and the solid residues were recrystallized from ethanol-*N,N'*-dimethyl formamide (DMF) to give yellow solid, yield 68 %; mp 193–195 °C; ^1H NMR (300 MHz, CDCl₃/TMS) δ : 3.96 (s, 3H), 3.98 (s, 6H), 6.95 (s, 2H), 7.39 (d, J =9.0 Hz, 1H), 7.65 (t, J =8.1 Hz, 1H), 7.76–7.95 (m, 3H), 8.02 (d, J =15.6 Hz, 1H), 8.14 (d, J =9.0 Hz, 1H), 8.43 (d, J =8.1 Hz, 1H), 9.44 (s, 1H). ^{13}C NMR (75 MHz, CDCl₃/TMS) δ : 56.22, 61.05, 106.05, 113.21, 116.57, 121.85, 123.31, 123.37, 126.70, 129.24, 129.81, 130.30, 130.43, 136.23, 144.09, 145.13, 153.42, 186.30. ESI-MS m/z : 416.9 (M + H) $^+$. Anal. calcd for C₂₅H₂₀O₆: C 72.11, H 4.84; found: C 72.19, H 4.97.

3-(3-(3,4,5-Trimethoxyphenyl)-prop-2-enoyl)-2H-1-benzopyran-2-one (1d)

A mixture of 3-acetyl-2H-1-benzopyran-2-one (376 mg, 2 mmol), 3,4,5-trimethoxybenzaldehyde (392 mg, 2 mmol) and piperidine (0.5 mL) in anhydrous ethanol (30 mL) was heated under reflux for 5 h. After cooling, the solvent was removed under reduced pressure and the solid residues were recrystallized from ethanol-DMF to give yellow solid, yield 59 %; mp 162–164 °C; ^1H NMR (300 MHz, CDCl₃/TMS) δ : 3.92 (s, 3H), 3.94 (s, 3H), 6.92 (s, 2H), 7.35–7.44 (m, 2H), 7.65–7.72 (m, 2H), 7.80 (d, J =15.6 Hz, 1H), 7.87 (d, J =15.6 Hz, 1H), 8.61 (s, 1H). ^{13}C NMR (75 MHz, CDCl₃/TMS) δ : 56.22, 61.03, 106.06, 116.73, 118.58, 123.20, 125.04, 125.36, 130.05, 130.31, 134.27, 145.23, 148.07, 153.43, 155.22, 159.45, 186.32. ESI-MS m/z : 367.1 (M + H) $^+$. Anal. calcd for C₂₁H₁₈O₆: C 68.85, H 4.95; found: C 68.81, H 5.01.

3-(3-(2,4-dimethoxyphenyl)-prop-2-enoyl)-2H-1-benzopyran-2-one (1e)

A mixture of 3-acetyl-2H-1-benzopyran-2-one (376 mg, 2 mmol), 2,4-dimethoxy benzaldehyde (332 mg, 2 mmol) and piperidine (0.5 mL) in anhydrous ethanol (30 mL) was heated under reflux for 5 h. After cooling, the solvent was removed under reduced pressure and the solid residues were recrystallized from ethanol-DMF to give yellow solid, yield 69 %; mp 185–187 °C; ^1H NMR (300 MHz, CDCl₃/TMS) δ : 3.87 (s, 3H), 3.91 (s, 3H), 6.45 (d, J =2.1 Hz, 1H), 6.54 (dd, J =8.4, 2.1 Hz, 1H), 7.32–7.41 (m, 2H), 7.62–7.69 (m, 3H), 7.90 (d, J =15.6 Hz, 1H), 8.18 (d, J =15.6 Hz, 1H), 8.55 (s, 1H). ^{13}C NMR (75 MHz, CDCl₃/TMS) δ : 55.53, 55.57, 98.34, 105.52, 116.64, 117.11, 118.69, 121.89, 124.85, 126.00, 129.87, 131.16, 133.85, 140.76, 147.38, 155.11, 159.37, 160.71, 163.47, 186.77. ESI-MS m/z : 337.1 (M + H) $^+$. Anal. calcd for C₂₀H₁₆O₅: C 71.42, H 4.79; found: C 71.54, H 4.86.

3-(3-(2-fluorenyl)-prop-2-enoyl)-2H-1-naphtho[2,1-b]pyran-2-one (1f)

A mixture of ANPO (476 mg, 2 mmol), 2-fluorene-carboxaldehyde (388 mg, 2 mmol) and piperidine (0.5 mL) in anhydrous ethanol (30 mL) was heated under reflux for 5 h. After cooling, the solvent was removed under reduced pressure and the solid residues were recrystallized from ethanol-DMF to give yellow solid, yield 71 %; mp 241–243 °C; ^1H NMR (300 MHz, CDCl₃/TMS) δ : 3.93 (s, 2H), 7.31–7.41 (m, 2H), 7.50 (d, J =9.0 Hz, 1H), 7.55–7.64 (m, 2H), 7.68–7.94 (m, 6H), 8.01 (d, J =15.6 Hz, 1H), 8.09 (d, J =9.0 Hz, 1H), 8.15 (d, J =15.6 Hz, 1H), 8.41 (d, J =8.4 Hz, 1H), 9.41 (s, 1H). ^{13}C NMR (75 MHz, CDCl₃/TMS) δ : 36.79, 113.21, 116.56, 120.22, 120.49, 121.86, 123.09, 123.37, 125.12, 125.20, 126.64, 126.99, 127.61, 128.81, 129.18, 129.23, 129.81, 130.27, 133.51, 136.11, 140.89, 143.81, 144.02, 144.10, 144.65, 145.59, 156.04, 159.64, 186.23. ESI-MS m/z : 415.0 (M + H) $^+$. Anal. calcd for C₂₉H₁₈O₃: C 84.04, H 4.38; found: C 84.16, H 4.32.

3-(3-(2-fluorenyl)-prop-2-enoyl)-2H-1-benzopyran-2-one (1g)

A mixture of 3-acetyl-2H-1-benzopyran-2-one (376 mg, 2 mmol), 2-fluorene-carboxaldehyde (388 mg, 2 mmol) and piperidine (0.5 mL) in anhydrous ethanol (30 mL) was heated under reflux for 5 h. After cooling, the solvent was removed under reduced pressure and the solid residues were recrystallized from ethanol-DMF to give yellow solid, yield 75 %; mp 222–224 °C; ^1H NMR (300 MHz, CDCl₃/TMS) δ : 3.98 (s, 2H), 7.37–7.45 (m, 4 H), 7.60 (d, J =6.9 Hz, 1H), 7.66–7.72 (m, 3 H), 7.83 (d, J =8.1 Hz, 2 H), 7.92 (s, 2 H),

7.98 (d, $J=15.9$ Hz, 1H), 8.05 (d $J=15.6$ Hz, 1H), 8.64 (s, 1H). ^{13}C NMR (75 MHz, CDCl_3/TMS) δ : 36.80, 116.73, 118.63, 120.24, 120.51, 123.00, 124.99, 125.13, 125.22, 127.01, 127.65, 128.78, 130.05, 133.39, 134.21, 143.83, 144.10, 145.71, 148.08, 155.25, 186.33. ESI-MS m/z : 365.1 ($\text{M} + \text{H}$) $^+$. Anal. calcd for $\text{C}_{25}\text{H}_{16}\text{O}_3$: C 82.40, H 4.43; found: C 82.36, H 4.49.

3-(3-(9-anthryl)-prop-2-enoyl)-2 H-1-naphtho[2,1-b]pyran-2-one (1h)

A mixture of ANPO (476 mg, 2 mmol), 9-anthraldehyde (412 mg, 2 mmol) and piperidine (0.5 mL) in anhydrous ethanol (30 mL) was heated under reflux for 5 h. After cooling, the solvent was removed under reduced pressure and the solid residues were recrystallized from ethanol-DMF to give red crystals, yield 78 %; mp 233–235 °C; ^1H NMR (300 MHz, CDCl_3/TMS) δ : 7.50–7.69 (m, 6H), 7.82 (t, $J=8.4$ Hz, 1H), 7.97 (d, $J=7.5$ Hz, 1H), 8.01 (d, $J=15.9$ Hz, 1H), 8.05 (d, $J=8.2$ Hz, 2H), 8.14 (d, $J=9.0$ Hz, 1H), 8.44–8.50 (m, 4H), 8.93 (d, $J=16.2$ Hz, 1H), 9.50 (s, 1H). ^{13}C NMR (75MHz, CDCl_3/TMS) δ : 113.18, 116.63, 121.83, 123.54, 125.46, 126.58, 126.71, 128.90, 129.29, 129.74, 129.82, 129.91, 130.31, 131.31, 132.81, 136.32, 141.56, 144.20, 156.21, 159.49, 162.33, 186.66. ESI-MS m/z : 427.1 ($\text{M} + \text{H}$) $^+$. Anal. calcd for $\text{C}_{30}\text{H}_{18}\text{O}_3$: C 84.49, H 4.25; found: C 84.53, H 4.33.

Results and Discussion

Absorption Spectra

UV–vis absorption spectra of these molecules in THF or dichloromethane (DCM) solutions are given in Fig. 2, and the UV data are summarized in Table 1. Clearly, these organic dyes demonstrate maximum absorption bands at 368–406 nm, and an increase in the absorption maximum values is seen as we go through the series **1d** (368 nm) < **1g** (381 nm) < **1e** (385 nm) < **1b** (391 nm) < **1a** (401 nm) < **1h** (402 nm) < **1c** (403 nm) < **1f** (406 nm). Therefore, among these molecules, **1d** has the shortest absorption wavelength.

As shown in Fig. 2a, in THF solution (2.52×10^{-5} M), the absorption spectrum of the intermediate ANPO exhibited two absorption maxima at 337 and 380 nm, which are in good agreement with those of literature report (337 and 382 nm, in acetonitrile) [16]. The absorption peak at the longer wavelength can be assigned to π - π transition. In comparison with the intermediate ANPO, the maxima absorption wavelengths of all five benzocoumarins (**1a–1c**, **1f** and **1h**) displayed a red-shift of 11–26 nm. Moreover, these bathochromic shifts may be ascribed to the inductive effects of the chalcone moiety and the substituents. Additionally,

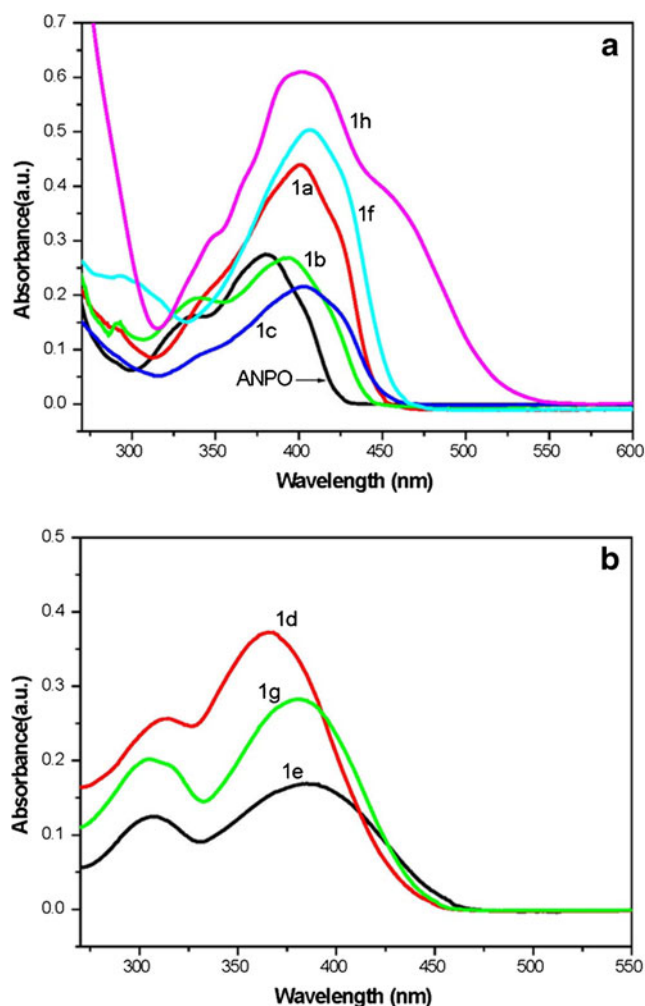


Fig. 2 Absorption spectra of the coumarin-based fluorophores

Table 1 Optical properties of the coumarin-based fluorophores

Compounds	Concentration 10^{-5} M	$\lambda_{\text{max}}(\text{abs})^{\text{a}}$ nm	$\epsilon \times 10^4$ $\text{M}^{-1} \text{cm}^{-1}$ ^b	$\lambda_{\text{max}}(\text{em})^{\text{c}}$ nm
1a	2.18	401	2.02	595
1b	2.27	391	1.18	532
1c	2.17	403	0.99	532
1d	2.45	368	1.52	532
1e	1.85	385	0.92	557 ^d
1f	2.13	406	2.36	545
1g	2.15	381	1.31	520 ^d
1h	2.02	402	3.02	645

^a Measured in THF solution for **1a** and **1b**, and in CH_2Cl_2 solution for the rest

^b Molar absorption coefficient

^c Measured in the solid state excited by 325 nm He–Cd laser

^d Measured in the solid state excited by 385 nm light from a Xe lamp

three coumarins, **1d**, **1e** and **1g**, have the very similar spectral shape, and exhibit two maxima, one of low intensity at short wave length (~310 nm) and one of high intensity at longer wave length (368–385 nm) (Fig. 2b). Particularly, the two absorption peaks at 306 and 381 nm for **1g** are almost identical to those of the fluorene–coumarin hybrid, ethyl 8-methoxy-6-(2-fluorenyl) azo-2*H*-1-benzopyran-2-one-3-carboxylate (**MFBC**), with two maximum centered at 306 nm and 377 nm [13].

By comparing the absorption spectra of these molecules, it can be seen that the benzocoumarin system caused a bathochromic effect of approximately 25–35 nm in λ_{\max} relative to the coumarin system. Concomitantly, the replacement of a boronophenyl group with a boronothienyl unit resulted in a small red shift of approximately 10 nm in λ_{\max} . Further, when replacing boronophenyl with a 3,4,5-trimethoxyphenyl, 2-fluorenyl or 9-anthryl donors, a red shift of approximately 11–15 nm in λ_{\max} is observed. Thus it appears that more π -electrons and more extended π -conjugated system may be involved in **1f** than those in the other samples. This may be related to the stronger electronic effect of the end benzocoumarin and fluorene units.

Photoluminescence Spectra of the Benzocoumarins (**1a–1c**, **1f** and **1h**)

The solid-state photoluminescence of the benzocoumarins (**1a–1c**, **1f** and **1h**) were examined with a helium–cadmium laser of 325 nm at room temperature. The photoluminescence of 3-(3-(4-*N,N*-diphenylaminophenyl)prop-2-enoyl)-2*H*-1-naphtho[2,1-*b*]pyran-2-one (**DPNPO**), which was previously reported by us [12], is also discussed for comparative purposes. As shown in Fig. 3, all the studied chromophores are fluorescent in solid-state, though **1a** has low emission intensity. These compounds have their maximum emission peaks located at 532–645 nm (Table 1), indicating that they can emit green to red lights. Moreover, the structural modification obviously causes difference in fluorescence peak intensity.

Among six benzocoumarins, only compound **1a** displays two emission peaks at near 520 and 595 nm with a shoulder at 640 nm, roughly corresponding to green and yellow light. In comparison with **1a**, the benzocoumarins (**1b**, **1c**, **1f** and **1h**) exhibit a very different emission, and present a broad emission band when in the solid state. Moreover, the emission peaks of these benzocoumarins undergo a red-shift from **1b,1c** (532 nm) to **1f** (545 nm), **DPNPO** (595 nm) and to **1h** (645 nm). Therefore, the luminescent color could be turned, from green to red (Fig. 3), by introducing different functional groups into benzocoumarin unit. For instance, as mentioned above, **1c** emits a strong green light at 532 nm, while **1f** presents a yellow-green emission at 545 nm. The

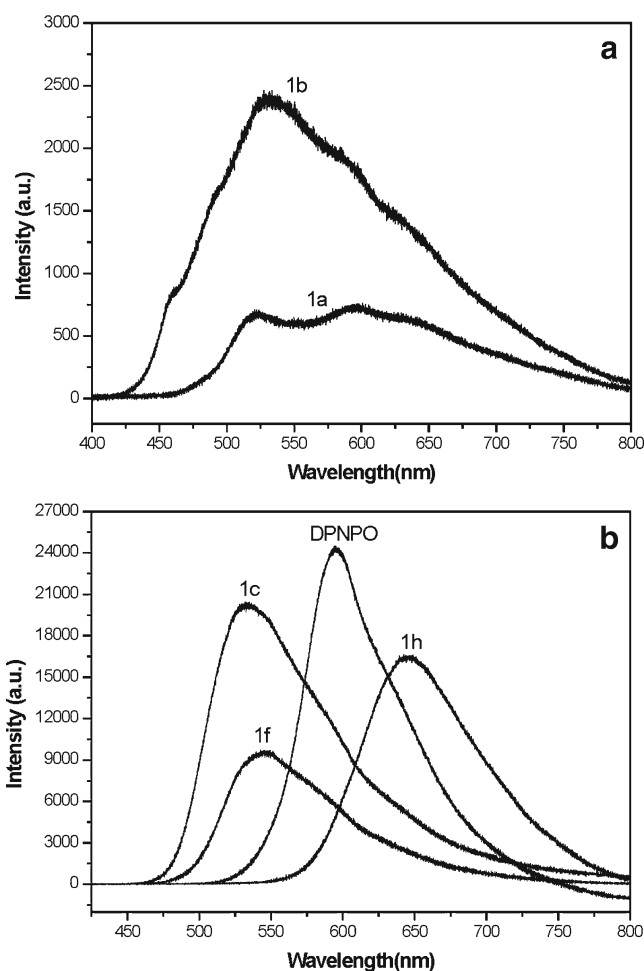


Fig. 3 Photoluminescence spectra of the benzocoumarins in the solid state

replacement of the 3,4,5-trimethoxyphenyl group with a triphenylamine group resulted in a red-shifted to 595 nm of the emission spectra for **DPNPO** as compared to **1c**. Further structural modification gave a brighter red light emission at 645 nm for **1h** when the 3,4,5-trimethoxyphenyl group was replaced by a 9-anthryl group. On the basis of the above results, it can be concluded that the nature of the substituents have significant influences on the solid-state luminescent properties, and the emission color can be tuned from green to red by structural modification.

Fluorescence Enhancement Behaviour of **1b**

The fluorescence behaviour of **1b** was further studied in a mixture of water/THF under different water fractions. Changes in the photoluminescence peak intensities versus water fraction of the mixture for compound **1b** were plotted, as shown in Fig. 4. When the dilute THF solution of **1b** was excited at 391 nm, only very weak signal was recorded. As the water fraction increased, the change of fluorescence

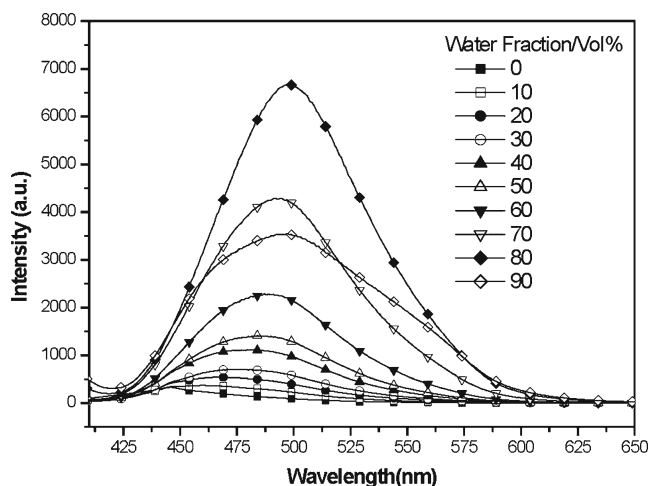
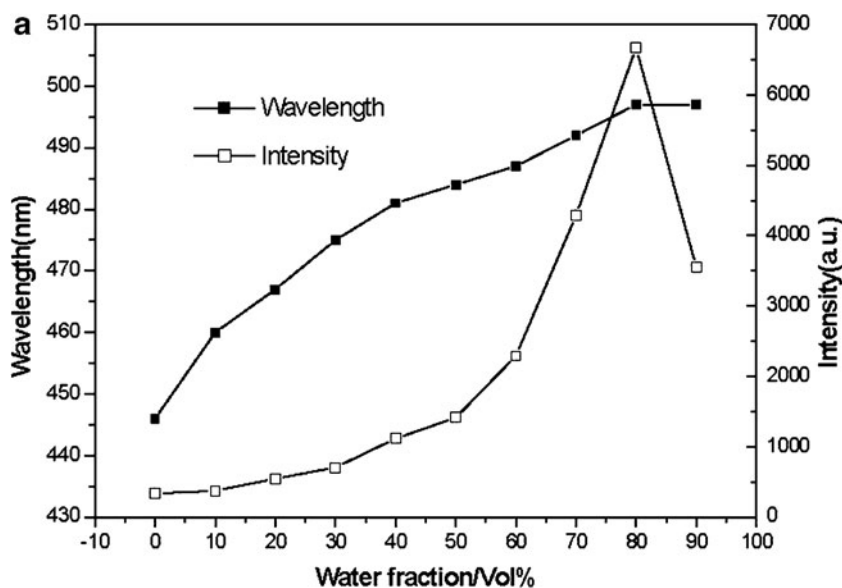


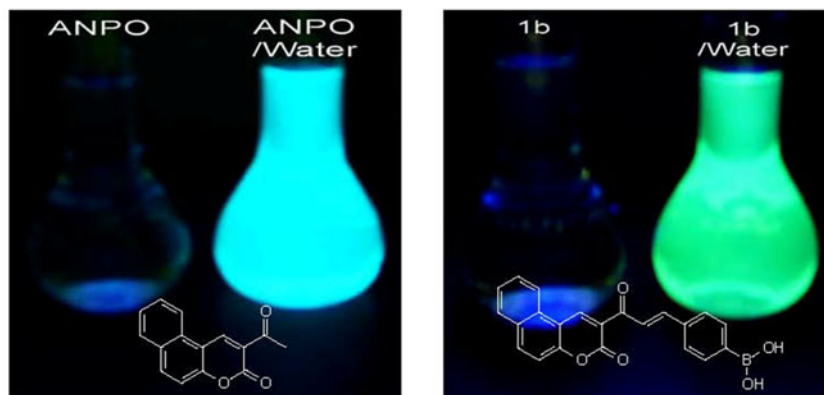
Fig. 4 Photoluminescence spectra of **1b** in THF with different water fraction (1.14×10^{-5} M)

emission intensity exhibited a two-step process: first enhanced, and then reduced (Fig. 5a). Concomitantly, a red

Fig. 5 a Photoluminescence wavelength and intensity of **1b** in THF with different water fraction. **b** Photographs for ANPO (left) and **1b** (right) in THF with and without addition of water under irradiation at 365 nm



b



shift in the fluorescence emission maximum was observed (Fig. 5a). When the water fraction was increased from 0 to 30 %, the fluorescence intensity of **1b** was slightly enhanced and its fluorescence emission maximum (446 nm) was red-shifted by 29 nm to 475 nm. Upon the increasing of water content from 40 to 80 %, **1b** shows a strong blue-green fluorescence emission peak with a significant fluorescence enhancement and a red shift in its emission wavelength (from 481 to 497 nm). However, a significant drop in the overall intensity is observed when the water fraction was further increased from 80 to 90 %. Moreover, its emission maximum is maintained (497 nm). Thus, more than 80 % water content is not effective in enhancing the fluorescence properties.

It is noteworthy that similar emission enhancement was also observed in the behaviour of its parent ANPO. In the THF/water mixtures with high fractions of water (70 %), ANPO emits intense blue fluorescence (Fig. 5b), with the peak maxima at 466 nm, which is obviously blue-shifted by 29 nm compared to that of **1b**.

The increase in fluorescence intensity for **1b** was considered to be a result of the aggregation-induced emission enhancement effect. Since the compound **1b** is insoluble in water, the molecule has aggregated into solid particles in the THF/water mixtures with high water contents. This phenomenon was often observed in some compounds with aggregation-induced emission enhancement properties [17,18]. Another reason of the fluorescence enhancement may be attributed to the solvation, which caused the change in the microscopic polarity around the fluorophore with increasing concentrations of water in THF. However, more experiments must be carried out to estimate such hypothesis.

Additionally, it should be pointed out that the significant difference in the position of the emission maxima between in the aggregate state (497 nm) and in the pure THF solution (446 nm) or in the solid state (532 nm) may be attributed to several factors, such as the molecular shape, packing structure, the intermolecular interactions, organizational morphology and the excitation wavelength and the excitation power.

Second-Order Nonlinear Optical Properties of **1d**

The solid-state optical properties of **1d** were also investigated with laser pulses. Figure 6 shows the solid-state luminescence spectrum of **1d** under 325 nm light excitation. Intriguingly, based on the observation data, it could be found that the sample exhibits intense green emission at 532 nm, which is identical to the emission maximum of **1c** in the solid state. However, compounds **1e** and **1g** show peak emissions at 557 and 520 nm, respectively, when in the solid state (Table 1).

In view of the possible importance of the strong green solid-state emission of **1d** with the shortest absorption

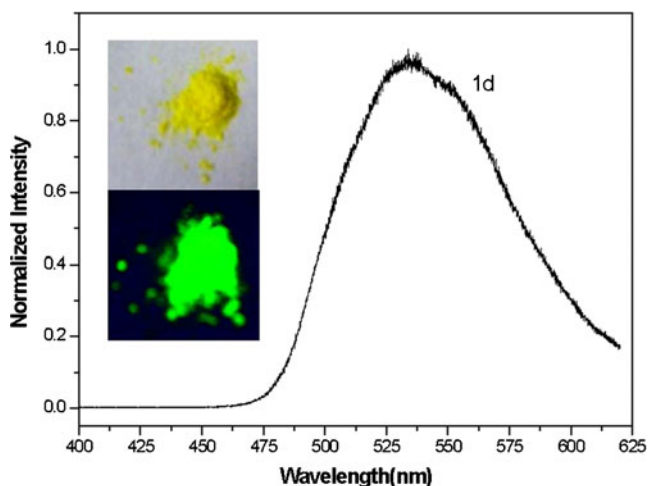


Fig. 6 Photoluminescence spectra of **1d** in the solid state. *Inset*: Photographs for **1d** in solid state under room light (*top*) and under 365 nm UV light (*bottom*)

wavelength and the continued interest in the development of nonlinear optical materials, the second-order nonlinear optical responses of **1d** was studied by the Kurtz powder method [19] using a Q-switched Nd: YAG laser of 1064 nm wavelength. At the same time, potassium dihydrogen phosphate (KDP), a well known nonlinear optical material for various optoelectronics applications [20], was used as a reference material in the second harmonic generation (SHG) measurement. Figure 7 shows the second-harmonic intensity as a function of incident fundamental intensity, and SHG photographs under 1064 nm light excitation. When the powdered sample **1d** is pumped at 1064 nm, strong green emission associated to SHG can be clearly seen by naked eyes, as shown in Fig. 7. In contrast, KDP just emits very weak green light. Preliminary experimental results indicated that the SHG efficiency from **1d** is 5.8 times more intense than that of KDP (1064 nm). Further research on phase matching studies of the sample is currently under way in our laboratory.

Conclusions

In summary, we have presented the synthesis, characterization and photoluminescence properties of some coumarin-based fluorophores. The benzocoumarins show solid-state emissions, varying from green to red depending on the molecular structures. In particular, **1b** exhibits interesting fluorescence responses to water. Moreover, **1d** displays a bright green emission at 532 nm and relatively high SHG efficiency than that of KDP. These compounds are highly promising candidates for applications in optoelectronic devices, solid-state lighting technologies and nonlinear optics.

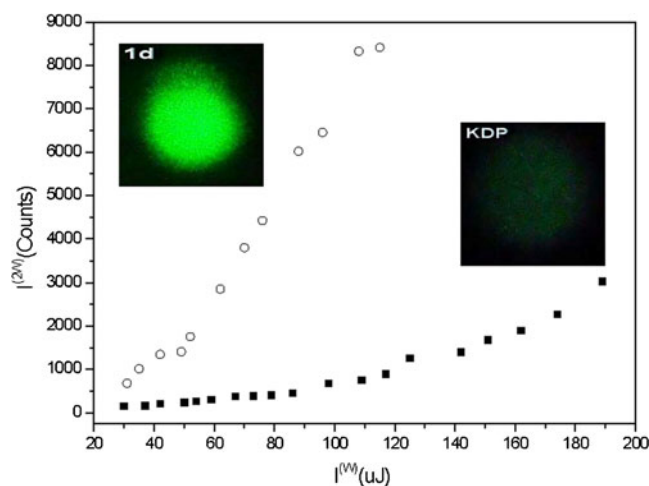


Fig. 7 Second harmonic intensity as a function of incident fundamental intensity for **1d** and KDP. *Inset*: SHG Photographs for **1d** and KDP under 1064 nm light excitation

Acknowledgments This work is supported by the Nature Science Foundation of Shandong Province of China (No. ZR2010BM032).

References

1. Kontogiorgis CA, Hadjipavlou-Litina DJ (2005) Synthesis and anti-inflammatory activity of coumarin derivatives. *J Med Chem* 48(20):6400–6408
2. Hamdi N, Puerta MC, Valerga P (2008) Synthesis, structure, antimicrobial and antioxidant investigations of dicoumarol and related compounds. *Eur J Med Chem* 43:2541–2548
3. Matos MJ, Vina D, Queaada E, Picciau C, Delogu G, Orallo F (2009) A new series of 3-phenylcoumarins as potent and selective MAO-B inhibitors. *Bioorg Med Chem Lett* 19:3268–3270
4. Liu XG, Cole JM, Waddell PG, Lin TC, Radia J, Zeidler A (2012) Molecular origins of optoelectronic properties in coumarin dyes: toward designer solar cell and laser applications. *J Phys Chem A* 116:727–737
5. Kim TK, Lee DN, Kim HJ (2008) Highly selective fluorescent sensor for homocysteine and cysteine. *Tetrahedron Lett* 49:4879–4881
6. Fu Q, Cheng LL, Zhang Y, Shi WF (2008) Preparation and reversible photo-crosslinking/photo-cleavage behavior of 4-methylcoumarin functionalized hyperbranchedpolyester. *Polymer* 49:4981–4988
7. Yu TZ, Zhang P, Zhao YL, Zhang H, Meng J, Fan DW (2009) Synthesis and photoluminescent properties of two novel tripodal compounds containing coumarin moieties. *Spectrochim Acta A: Mol Biomol Spectrosc* 73:168–173
8. Turki H, Abid S, Fery-Forgues S, Gharbi RE (2007) Optical properties of new fluorescent iminocoumarins: part 1. *Dyes Pigm* 73:311–316
9. Kim HM, Fang XZ, Yang PR, Yi JS, Ko YG, Piao MJ (2007) Design of molecular two-photon probes for in vivo imaging. 2H-Benzo[h]chromene-2-one derivatives. *Tetrahedron Lett* 48:2791–2795
10. Asiri AM, Khan SA (2011) Synthesis, characterization and optical properties of mono- and bis-chalcone. *Mater Lett* 65:1749–1752
11. Qiao ZT, Wang Q, Zhang FL, Wang ZL, Bowling T, Nare B, Jacobs RT, Zhang J, Ding DZ, Liu YG, Zhou HC (2012) Chalcone – Benzoxaborole hybrid molecules as potent antitrypanosomal agents. *J Med Chem* 55:3553–3557
12. Sun YF, Cui YP (2008) The synthesis, characterization and properties of coumarin-based chromophores containing a chalcone moiety. *Dyes Pigm* 78:65–76
13. Sun YF, Xu SH, Chen ZY, Pan WL, Song HC, Chen JH (2011) Broadband luminescence and emission enhancement. *Color Technol* 127:328–334
14. Sun YF, Xu SH, Wu RT, Wang ZY, Zheng ZB, Li JK, Cui YP (2010) The synthesis, structure and photoluminescence of coumarin-based chromophores. *Dyes Pigm* 87:109–118
15. DiCesare N, Lakowicz JR (2002) Chalcone-analogue fluorescent probes for saccharides signaling using the boronic acid group. *Tetrahedron Lett* 43:2615–2618
16. Murata C, Masuda T, Kamochi Y, Todoroki K, Yoshida H, Nohta H, Yamaguchi M, Takadate A (2005) Improvement of fluorescence characteristics of coumarins: syntheses and fluorescence properties of 6-methoxycoumarin and benzocoumarin derivatives as novel fluorophores emitting in the longer wavelength region and their application to analytical reagents. *Chem Pharm Bull* 53:750–758
17. Li HY, Chi ZG, Xu BJ, Zhang XQ, Yang ZY, Li XF, Liu SW, Zhang Y, Xu JR (2010) New aggregation-induced emission enhancement materials combined triarylamine and dicarbazolyl triphenylethylene moieties. *J Mater Chem* 20:6103–6110
18. Zhang XQ, Chi ZG, Xu BJ, Li HY, Yang ZY, Li XF, Liu SW, Zhang Y, Xu JR (2011) Synthesis of blue light emitting bis(triphenylethylene) derivatives: a case of aggregation-induced emission enhancement. *Dyes Pigm* 89:56–62
19. Kurtz SK, Perry TT (1968) A powder technique for the evaluation of nonlinear optical materials. *J Appl Phys* 39:3798–3813
20. Podder J (2002) The study of impurities effect on the growth and nucleation kinetics of potassium dihydrogen phosphate. *J Crystal Growth* 237–239:70–75